Investigation of the Ultradrawing Properties of Gel Spun Fibers of Ultra-High Molecular Weight Polyethylene/Carbon Nanotube Blends

Jen-Taut Yeh,[1,2,3] Shui-Chuan Lin,[1] Kan-Nan Chen,[4] Kuo-Shien Huang[5]

[1]*Graduate School of Polymer Engineering, National Taiwan University of Science and Technology, Taipei, Taiwan*
[2]*Faculty of Chemistry and Material Science, Hubei University, Wuhan, People's Republic of China*
[3]*Institute of Textile and Material Wuhan University of Science and Engineering, Wuhan, China*
[4]*Department of Chemistry, Tamkang University, Taipei county, Taiwan*
[5]*Department of Polymer Materials, Kun Shan University, Tainan county, Taiwan*

Received 8 January 2008; accepted 11 April 2008
DOI 10.1002/app.28663
Published online 18 August 2008 in Wiley InterScience (www.interscience.wiley.com).

ABSTRACT: The carbon nanotubes (CNTs) contents, ultrahigh-molecular-weight polyethylene (UHMWPE) concentrations and temperatures of UHMWPE, and CNTs added gel solutions exhibited significant influence on their rheological and spinning properties and the drawability of the corresponding UHMWPE/CNTs as-prepared fibers. Tremendously high shear viscosities (ηs) of UHMWPE gel solutions were found as the temperatures reached 140°C, at which their ηs values approached the maximum. After adding CNTs, the ηs values of UHMWPE/CNTs gel solutions increase significantly and reach a maximum value as the CNTs contents increase up to a specific value. At each spinning temperature, the achievable draw ratios obtained for UHMWPE as-prepared fibers prepared near the optimum concentration are significantly higher than those of UHMWPE as-prepared fibers prepared at other concentrations. After addition of CNTs, the achievable draw ratios of UHMWPE/CNTs as-prepared fibers prepared near the optimum concentration improve consistently and reach a maximum value as their CNTs contents increase up to an optimum value. To understand these interesting drawing properties of the UHMWPE and UHMWPE/CNTs as-prepared fibers, the birefringence, thermal, morphological, and tensile properties of the as-prepared and drawn fibers were investigated. Possible mechanisms accounting for these interesting properties are proposed. © 2008 Wiley Periodicals, Inc. J Appl Polym Sci 110: 2538–2548, 2008

Key words: UHMWPE/CNTs; shear viscosities; achievable draw ratio; birefringence; morphology

INTRODUCTION

The unprecedented physical and chemical properties of carbon nanotubes (CNTs) have created enormous attraction because they were first discovered by Iijima in 1991.[1] They are well known for enormous aspect ratio, high elastic modulus, low density, and fierce resistance to failure, which make them ideal as reinforcement for polymer composites. Incorporation of uniformly dispersed and aligned CNTs in polymer matrix can provide polymer composites with dramatically improved strength and modulus in their machine direction. These expectations have recently been confirmed by a number of studies.[2–8] Andrew et al.[2] reported that the tensile strength, modulus, and electrical conductivity of a pitch composite fiber with 5 wt % loading of purified single-walled carbon nanotubes (SWNTs) are enhanced by about 90, 150, and 340%, respectively, as compared to the corresponding values of unmodified isotropic pitch fibers. On the other hand, by well-dispersing 1 wt % purified multiwall carbon nanotubes (MWCNTs) in polystyrene (PS) solutions, the elastic modulus and break stress of the solution-casted MWCNTs/PS films increase by about 40 and 25%, respectively.[3]

Recently, polyvinyl alcohol (PVA)/CNTs[5,6] and ultra-high molecular weight polyethylene (UHMWPE)/CNTs[6–8] composite fibers have attracted significant attention, because the stresses applied during gel spinning can align the nanotubes along the fiber longitudes. Similar improvements in tensile and bending properties were found in CNTs-containing PVA[4,5] or UHMWPE composite fiber specimens.[6–8] By using 0.35 wt % nanotubes and 1.0 wt % dispersing surfactant of sodium dodecyl sulfate, the SWCNTs-containing PVA fibers can be strongly bent without breaking. Their elastic modulus is 10 times

Correspondence to: J.-T. Yeh (jyeh@tx.ntust.edu.tw).
Contract grant sponsor: Department of Industrial Technology, Ministry of Economic Affairs; contract grant number: 95-EC-17-A-11-S1-057.
Contract grant sponsor: National Science Council; contract grant number: NSC 95-2221-E-253-008-MY3.

higher than the modulus of high-quality bucky paper. Dalton et al.[5] further reported for preparation of the "supertough" PVA/CNTs fiber through a coagulation-based spinning method. Most recently, as reported by Ruan et al.,[8] the tensile strength and elongation at break of 5 wt % MWCNTs filled UHMWPE gel-spun composite fiber specimen can reach 4.2 GPa and 5%, respectively, which are 18.8 and 15.4% higher than that of the pure UHMWPE fiber with the same draw ratios, respectively. On the other hand, the tensile strength and modulus of 1 wt % MWCNTs added UHMWPE composite fiber improved by 9 and 14% in comparison with those of the UHMWPE fibers, respectively.[7]

However, the tensile properties of theses CNTs-containing composite fibers described above only have limited improvement. The reinforcing efficiency of CNTs in composite applications depends strongly on the uniform dispersion of CNTs throughout the polymer matrix without destroying the integrity of the nanotubes. Moreover, a good interfacial adhesion or physical winding of polymer molecules on CNTs is required to achieve for load transfer across the polymer-CNTs interface and avoid intertube slippage within bundles. However, chemical modification of the surfaces of CNTs can introduce defects, destroy the integrity, and significantly reduce the mechanical properties of the CNTs,[9,10] although the modification can improve the dispersion of CNTs and their bonding into the polymer molecules. On the other hand, coagulation of CNTs in UHMWPE and/or PVA gel solutions can be encountered at high CNTs concentrations.

In contrast to the barely few studies on preparation of PVA/CNTs and UHMWPE/CNTs gel-spun fibers reported in the literature,[4–8] relatively low concentrations of "virgin" MWCNTs were sonicated and well-dispersed in UHMWPE gel solutions. Varying concentrations and compositions of UHMWPE/MWCNTs gel solutions were then gel-spun at different temperatures to improve the ultradrawing and tensile properties of the UHMWPE/CNTs composite fibers. The concentrations, compositions, and temperatures of ultrahigh-molecular-weight polyethylene and carbon nanotubes added gel solutions exhibited a significant influence on their rheological and spinning properties. Moreover, using optimum composition and spinning temperature of UHMWPE/CNTs gel solutions, the achievable draw ratio of UHMWPE/CNTs as-prepared fibers are significantly higher than those of the UHMWPE as-prepared fibers prepared at the optimum concentration and temperature. To understand these interesting drawing properties of the UHMWPE and UHMWPE/CNTs as-prepared fibers, the birefringences, thermal, morphological, and tensile properties of the as-prepared and drawn fibers were investigated. Possible mechanisms accounting for these interesting properties are proposed.

EXPERIMENTAL

Materials and sample preparation

The UHMWPE resin used in this study is associated with a weight-average molecular weight (M_w) of 5×10^6, which will be referred to as resin U in the following discussion. The carbon nanotubes (CNTs) used in this study will be called C, which are multiwall carbon nanotubes with diameters and lengths ranging from 40 to 60 nm and 0.5 to 500 μm, respectively. Resins U and CNTs were kindly supplied by Yung Chia Chemical Industrial Corp., Kaohsiung, Taiwan and by SNP Corp., Shenzhen, China, respectively. More than 95 wt % of purity, less than 3 wt % of amorphous carbon, and 0.2 wt % of ash (La, Ni) were quoted in the CNTs by SNP Corp. The specific surface areas of CNTs were quoted between 40 and 300 m^2/g. The CNTs were first mixed and ultrasonicated in decalin solution at 50°C for 1 h. The ultrasonicated and dispersed CNTs solutions were then mixed with U resin at varying weight ratio and concentrations at 150°C for 4 h, wherein 0.1 wt % of di-*t*-butyl-*p*-cresol was added as an antioxidant. The gel solutions prepared above were then fed into a temperature-controlled hopper and kept as hot homogenized solutions before further spinning. These prepared solutions were then gel-spun using a conical die with an exit diameter of 1 mm at an extrusion rate of 1000 mm/min and an extrusion temperature of 160, 170, and 180°C, respectively. A water bath and a winder with 70 mm in diameter were placed at a distance of 520 and 810 mm from the spinneret exit, respectively. The extruded gel fibers were cooled in a temperature-conditioned atmosphere and then quenched into a water bath for about 1 min, where the temperatures of the air atmosphere and water bath were controlled at 25°C. The quenched fibers were then extracted in a *n*-hexane bath for 5 min to remove the residual decalin solvent. The extracted fiber specimens were then dried in air for 30 min to remove the remaining hexane solvent before any drawing run. The compositions of the UHMWPE and UHMWPE/CNTs gel solutions and designations of the corresponding as-prepared fibers are summarized in Table I.

Viscosity measurements

A Brookfiled viscometer model LVDV-II+ was used to determine the shear viscosities of UHMWPE and CNTs-containing UHMWPE gel solutions prepared in the previous section. The solutions prepared at 80, 90, 100, 110, 120, 130, 140, 150, 160, 170, 180, 190, and 200°C were placed in a jacketed temperature-controlled cell for varying amounts of time before viscosity measurements were taken.

TABLE I
The Compositions of the UHMWPE and UHMWPE/CNTs Gel Solutions and Designations of the Corresponding As-Prepared Fibers Prepared in This Study

As-prepared fibers	Gel solutions	Solution temperatures (°C)	Concentrations (kg/m^3)	CNTs contents (wt %)
$F_{10}C_{0\text{-}160}$	$U_{10}C_0$	160	10	0
$F_{10}C_{0\text{-}170}$	$U_{10}C_0$	170	10	0
$F_{10}C_{0\text{-}180}$	$U_{10}C_0$	180	10	0
$F_{15}C_{0\text{-}160}$	$U_{15}C_0$	160	15	0
$F_{15}C_{0\text{-}170}$	$U_{15}C_0$	170	15	0
$F_{15}C_{0\text{-}180}$	$U_{15}C_0$	180	15	0
$F_{20}C_{0\text{-}160}$	$U_{20}C_0$	160	20	0
$F_{20}C_{0\text{-}170}$	$U_{20}C_0$	170	20	0
$F_{20}C_{0\text{-}180}$	$U_{20}C_0$	180	20	0
$F_{25}C_{0\text{-}160}$	$U_{25}C_0$	160	25	0
$F_{25}C_{0\text{-}170}$	$U_{25}C_0$	170	25	0
$F_{15}C_{0\text{-}160}$	$U_{15}C_0$	160	15	0
$F_{15}C_{0.0005\text{-}160}$	$U_{15}C_{0.0005}$	160	15	0.0005
$F_{15}C_{0.001\text{-}160}$	$U_{15}C_{0.001}$	160	15	0.001
$F_{15}C_{0.0015\text{-}160}$	$U_{15}C_{0.0015}$	160	15	0.0015
$F_{15}C_{0.002\text{-}160}$	$U_{15}C_{0.002}$	160	15	0.002
$F_{15}C_{0.0025\text{-}160}$	$U_{15}C_{0.0025}$	160	15	0.0025
$F_{15}C_{0.005\text{-}160}$	$U_{15}C_{0.005}$	160	15	0.005
$F_{25}C_{0\text{-}180}$	$U_{25}C_0$	180	25	0
$F_{30}C_{0\text{-}160}$	$U_{30}C_0$	160	30	0
$F_{30}C_{0\text{-}170}$	$U_{30}C_0$	170	30	0
$F_{30}C_{0\text{-}180}$	$U_{30}C_0$	180	30	0
$F_{20}C_{0\text{-}170}$	$U_{15}C_0$	170	20	0
$F_{20}C_{0.0005\text{-}170}$	$U_{20}C_{0.0005}$	170	20	0.0005
$F_{20}C_{0.001\text{-}170}$	$U_{20}C_{0.001}$	170	20	0.001
$F_{20}C_{0.0015\text{-}170}$	$U_{20}C_{0.0015}$	170	20	0.0015
$F_{20}C_{0.002\text{-}170}$	$U_{20}C_{0.002}$	170	20	0.002
$F_{20}C_{0.0025\text{-}170}$	$U_{20}C_{0.0025}$	170	20	0.0025
$F_{20}C_{0.005\text{-}170}$	$U_{20}C_{0.005}$	170	20	0.005
$F_{25}C_{0\text{-}180}$	$U_{25}C_0$	180	25	0
$F_{25}C_{0.0005\text{-}180}$	$U_{25}C_{0.0005}$	180	25	0.0005
$F_{25}C_{0.001\text{-}180}$	$U_{25}C_{0.001}$	180	25	0.001
$F_{25}C_{0.0015\text{-}180}$	$U_{25}C_{0.0015}$	180	25	0.0015
$F_{25}C_{0.002\text{-}180}$	$U_{25}C_{0.002}$	180	25	0.002
$F_{25}C_{0.0025\text{-}180}$	$U_{25}C_{0.0025}$	180	25	0.0025

Morphology, birefringence, and thermal analysis

To observe the morphology of CNTs present in the gel fibers during the drawing processes, the as-prepared and drawn gel fibers prepared at varying compositions and conditions were then etched with excess amount of fuming nitric acid to emphasize the CNTs and crystalline morphology of the fiber specimen. The amorphous regions of fiber specimens could be etched with ultrasonic generator at 300 W at 60°C. After the acid treatment for 6 h, the sample was washed by deionized water subsequently by boiling acetone, and then dried at room temperature. The dried etched specimens were then gold-coated and examined using a Joel JSM-5200 Scanning Electron Microscopy (SEM). Birefringence properties of the as-prepared and drawn gel fibers were measured using a polarizing microspectrometer Model TFM-120 AFT. The thermal behavior of all samples was performed on a Du Pont differential scanning calorimeter (DSC) model 2000. All scans were carried out at a heating rate of 20°C/min under flowing nitrogen at a flow rate of 25 mL/min. Samples weighing 0.5 and 15 mg were placed in the standard aluminum sample pans for determination of their melting temperatures and percentage crystallinity. The percentage crystallinity values of the specimens were estimated using baselines drawn from 40 to 170°C and a perfect heat of fusion of polyethylene of 293 J/g.[11]

Drawing and tensile properties of the gel fibers

The fiber specimens used in the drawing experiments were cut from the dried as-prepared fibers and then stretched on a Tension testing machine model RTA-1T equipped with a temperature-controlled oven. The dimensions of the gel-spun fibers are 30 mm in length, which were wound and clamped in a stretching device and then stretched at a crosshead speed of 20 mm/min and a constant

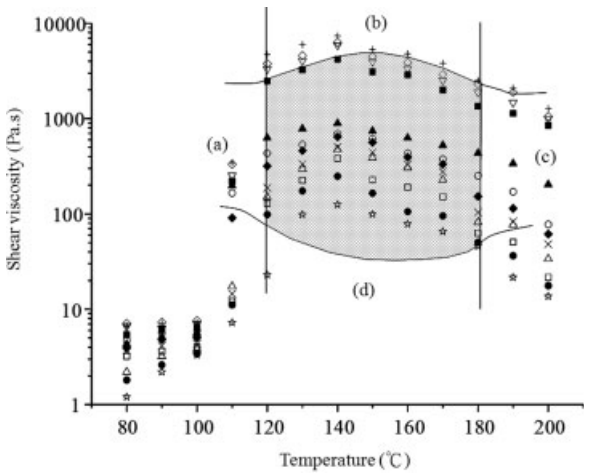

Figure 1 Shear viscosities of $U_{10}C_0$ (☆), $U_{10}C_{0.0002}$ (●), $U_{10}C_{0.002}$ (△), $U_{10}C_{0.005}$ (□), $U_{20}C_0$ (×), $U_{20}C_{0.0002}$ (◆), $U_{20}C_{0.002}$(▲), $U_{20}C_{0.005}$ (○), and $U_{40}C_0$ (■), $U_{40}C_{0.0002}$ (▽), $U_{40}C_{0.002}$ (+), $U_{40}C_{0.005}$ (◊) solutions at different temperatures. Regions (a), (b), (c), and (d) are inaccessible to spinning. The shadowed region represents the spinnable regions of the prepared solution.

temperature of 95°C. The draw ratio of each fiber specimen was determined as the ratio of the marked displacement after and before drawing. The marked displacement before drawing was 27 mm. The tensile properties of the as-prepared and drawn fibers were also determined using the Tension testing machine at a crosshead speed of 20 mm/min. A minimum of three samples of each specimen were tested and averaged during the tensile experiments.

RESULTS AND DISCUSSION

Shear viscosity and spinning properties of the gel solutions

The shear viscosities of UHMWPE and carbon nanotubes (CNTs) containing UHMWPE gel solutions with various compositions were summarized in Figure 1. As expected, higher shear viscosities were observed from higher concentration of the UHMWPE and CNTs-containing UHMWPE gel solutions at any fixed temperature above 80°C. However, at temperatures lower than 110°C, shear viscosity only slightly increased with the temperatures. At temperatures higher than 110°C, the shear viscosities of the UHMWPE and CNTs-containing gel solutions increased dramatically with the temperatures and reached the maximum value (η_{maxv}) when the temperature reached 140°C. For instance, the η_{maxv} values of the UHMWPE gel solutions increased significantly from 125.2 to 4189.6 Pa s as the concentration of UHMWPE solutions increased from 10 to 40 kg/m^3 (see Fig. 1). The shear viscosities then reduced significantly after the temperatures rose across 140°C. It is also worth noting that, at temperatures greater than 110°C, the shear viscosities of CNTs-containing UHMWPE gel solutions were significantly higher than those of base UHMWPE gel solutions with the same UHMWPE concentrations, respectively. In fact, the shear viscosities of CNTs-containing gel solutions increased significantly as their CNTs contents increased and reached an optimum value of 0.002 wt %. For instance, the shear viscosities of the $U_{10}C_x$, $U_{20}C_x$, and $U_{40}C_x$ series gel solutions at 140°C increased from 125.2 to 474.0, 504.4 to 895.2, and 4189.6 to 7401.6 Pa s, respectively, as their CNTs contents increased from 0 wt % to the optimum value of 0.002 wt %. However, the shear viscosities of the $U_{10}C_{0.005}$, $U_{20}C_{0.005}$, and $U_{40}C_{0.005}$ series gel solutions at 140°C reduced to 381.6, 695.8, and 6322.4 Pa s, respectively, when the CNTs content was 0.005 wt %.

It is not completely clear what accounts for these interesting shears viscosity properties of the UHMWPE and CNTs-containing UHMWPE gel solutions. However, the melting temperatures of most crystals present in the base UHMWPE resins are well above 110°C. The slightly melted UHMWPE crystals can not provide UHMWPE molecules enough interpenetrating mobility to form a stable but loosely entangled gel-network-structure in the UHMWPE and/or CNTs-containing UHMWPE gel solutions at these temperatures. This explains why shear viscosities of UHMWPE and CNTs-containing UHMWPE solutions prepared at temperatures lower than 110°C only slightly increased with temperature. In contrast, at temperatures between 120 and 140°C, significant amount of UHMWPE crystals can be melted to provide UHMWPE molecules enough interpenetrating mobility to form the stable entangled gel-network-structure in the solutions. Such inhomogeneous gel solutions were "solid-like" in nature and had the entangled gel-network-structure that showed tremendously high viscosities during the spinning process. Moreover, the dispersed CNTs with original lengths ranging from 0.5 to 500 μm can further reinforce the stable entangled gel-network-structures of the CNTs-containing UHMWPE solutions and hence, increase their shear viscosities with increasing CNTs contents. Consequently, the shear viscosity values of the UHMWPE and/or CNTs-containing UHMWPE gel solutions increased to the maximum as the temperatures reached 140°C, wherein the shear viscosities of the optimal 0.002 wt % CNTs-containing UHMWPE gel solutions (i.e., $U_{10}C_{0.002}$, $U_{20}C_{0.002}$, and $U_{40}C_{0.002}$) are about 278.6%, 77.5%, and 76.7% higher than those of the corresponding base UHMWPE gel solutions, respectively. However, the CNTs can coagulate when their contents in the gel solution became higher than a certain value. The coagulated CNTs

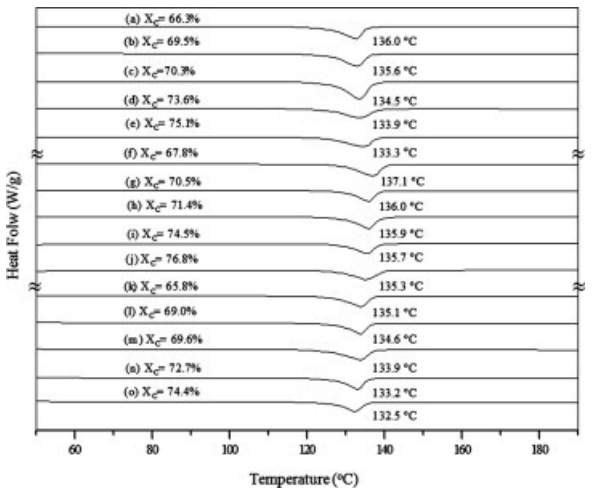

Figure 2 DSC thermograms of (a) $F_{15}C_{0\text{-}170}$, (b) $F_{15}C_{0.0005\text{-}170}$, (c) $F_{15}C_{0.001\text{-}170}$, (d) $F_{15}C_{0.002\text{-}170}$, (e) $F_{15}C_{0.005\text{-}170}$, (f) $F_{20}C_{0\text{-}170}$, (g) $F_{20}C_{0.0005\text{-}170}$, (h) $F_{20}C_{0.001\text{-}170}$, (i) $F_{20}C_{0.002\text{-}170}$, (j) $F_{20}C_{0.005\text{-}170}$, (k) $F_{25}C_{0\text{-}170}$, (l) $F_{25}C_{0.0005\text{-}170}$, (m) $F_{25}C_{0.001\text{-}170}$, (n) $F_{25}C_{0.002\text{-}170}$, and (o) $F_{25}C_{0.005\text{-}170}$ as-prepared fibers (X_c represents the percentage crystallinity values of the as-prepared UHMWPE fibers.).

may slide with each other and lead to a significant reduction in the measurements of shear viscosities. Based on these premises, it is reasonable to infer that the shear viscosity values of the CNTs-containing UHMWPE gel solutions can reduce significantly with increasing CNTs contents after it exceeds the optimal CNTs concentration value. However, completely melting of UHMWPE crystals followed by partial solvation of UHMWPE molecules can occur as the gel solution temperatures are well above 140°C. Under such circumstances, solvated UHMWPE molecules become more and more activated as the temperatures continue to increase. Moreover, thermal degradation of UHMWPE molecules could occur at relatively high temperatures during the preparation and spinning processes of UHMWPE gel solutions. Presumably, the overly activated and possibly thermal-degraded UHMWPE molecules are likely to facilitate the disentanglement of the gel-network-structure during the spinning process, and hence, cause a significant reduction in the shear viscosities of UHMWPE and/or CNTs-containing UHMWPE gel solutions when temperature rises across 140°C.

Finally, it is worth noting that only the UHMWPE and/or CNTs-containing UHMWPE gel solutions with shear viscosity values in the shadowed region of Figure 1 are spinnable. These gel solutions are associated with optimal shear viscosity values and have relatively good homogeneity. At temperatures lower than 120°C and/or solution concentrations lower than or equal to 10 kg/m^3, the shear viscosities of the prepared solutions are too low to spin stably [see Fig. 1(a,d)]. This is because the stable entangled gel-network-structure is not likely formed at these processing conditions. In contrast, at temperatures roughly between 120 and 150°C, the shear viscosities of the UHMWPE and CNTs-containing UHMWPE gel solutions are relatively high that makes the gel solutions un-spinnable [see Fig. 1(b)]. Moreover, at temperatures higher than 180°C, vaporization rates of the decalin solvent become too fast to keep the fully melted and overly activated gel solutions spinning in a stable manner [see Fig. 1(c)]. These spinning conditions and solution compositions associated with the regions outside of the spinnable shadowed region of Figure 1 are not suitable for spinning UHMWPE and/or UHMWPE/CNTs fibers in a stable manner, and are defined as the un-spinnable region.[12]

Thermal properties of the as-prepared fibers

Typical DSC thermograms and crystallinity values of the as-prepared UHMWPE and UHMWPE/CNTs fibers are summarized in Figures 2–4. A main melting endotherm was found on the DSC thermogram of the base UHMWPE as-prepared fiber (i.e., $F_{20}C_{0\text{-}170}$), wherein the percentage crystallinity and peak melting temperature values of the $F_{20}C_{0\text{-}170}$ as-prepared fiber are about 67.8% and 137.1°C, respectively, (see Fig. 2). After blending CNTs in UHMWPE gel solutions, the percentage crystallinity and melting temperature values of the $F_{20}C_{x\text{-}170}$ as-prepared fibers increase and reduce significantly as the CNTs contents increase, respectively. For

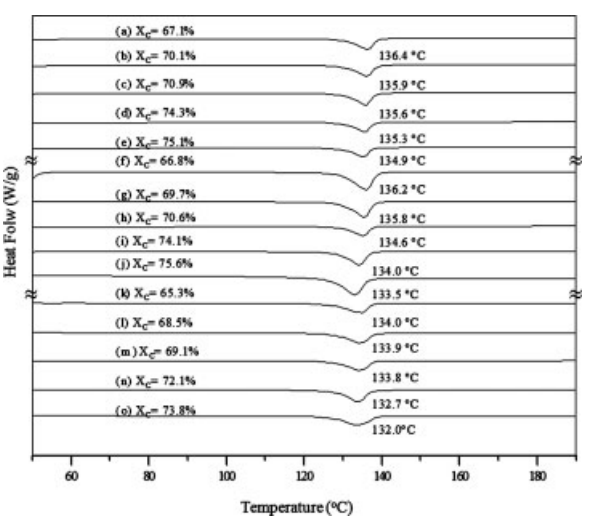

Figure 3 DSC thermograms of (a) $F_{15}C_{0\text{-}160}$, (b) $F_{15}C_{0.0005\text{-}160}$, (c) $F_{15}C_{0.001\text{-}160}$, (d) $F_{15}C_{0.002\text{-}160}$, (e) $F_{15}C_{0.005\text{-}160}$, (f) $F_{20}C_{0\text{-}160}$, (g) $F_{20}C_{0.0005\text{-}160}$, (h) $F_{20}C_{0.001\text{-}160}$, (i) $F_{20}C_{0.002\text{-}160}$, (j) $F_{20}C_{0.005\text{-}160}$, (k) $F_{25}C_{0\text{-}160}$, (l) $F_{25}C_{0.0005\text{-}160}$, (m) $F_{25}C_{0.001\text{-}160}$, (n) $F_{25}C_{0.002\text{-}160}$, and (o) $F_{25}C_{0.005\text{-}160}$ as-prepared fibers (X_c represents the percentage crystallinity values of the as-prepared UHMWPE fibers.).

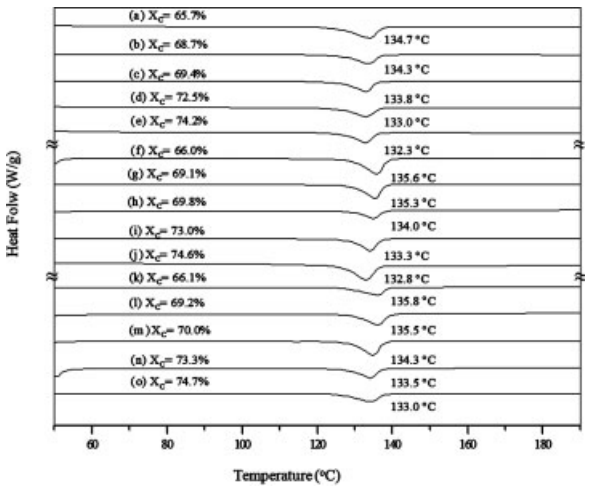

Figure 4 DSC thermograms of (a) $F_{15}C_{0\text{-}180}$, (b) $F_{15}C_{0.0005\text{-}180}$, (c) $F_{15}C_{0.001\text{-}180}$, (d) $F_{15}C_{0.002\text{-}180}$, (e) $F_{15}C_{0.005\text{-}180}$, (f) $F_{20}C_{0\text{-}180}$, (g) $F_{20}C_{0.0005\text{-}180}$, (h) $F_{20}C_{0.001\text{-}180}$, (i) $F_{20}C_{0.002\text{-}180}$, (j) $F_{20}C_{0.005\text{-}180}$, (k) $F_{25}C_{0\text{-}180}$, (l) $F_{25}C_{0.0005\text{-}180}$, (m) $F_{25}C_{0.001\text{-}180}$, (n) $F_{25}C_{0.002\text{-}180}$, and (o) $F_{25}C_{0.005\text{-}180}$ as-prepared fibers (X_c represents the percentage crystallinity values of the as-prepared UHMWPE fibers.).

instance, the percentage crystallinity values increase from 67.8 to 74.5 and 76.8%, but melting temperatures reduce from 137.1 to 135.7, and 135.3°C as the CNTs contents of $F_{20}C_{x\text{-}170}$ as-prepared fibers increase from 0 to 0.002 and 0.005 wt %, respectively. Similar CNTs content dependency of the percentage crystallinity and melting temperature values was found on other UHMWPE/CNTs fiber series spun at 170°C but different gel concentrations (i.e., $F_{15}C_{x\text{-}170}$ and $F_{25}C_{x\text{-}170}$ as-prepared fibers) (see Fig. 2) or spun at other temperatures (i.e., $F_{15}C_{x\text{-}160}$, $F_{20}C_{x\text{-}160}$, $F_{25}C_{x\text{-}160}$ and $F_{15}C_{x\text{-}180}$, $F_{20}C_{x\text{-}180}$, $F_{25}C_{x\text{-}180}$ as-prepared fibers) (see Figs. 3 and 4). The CNTs are well known for a large surface area per volume, which makes them in close proximity to a large fraction of the polymer matrix. Apparently, even small contents of carbon nanotubes can serve as efficient nucleation sites for UHMWPE molecules during the gel spinning process. These efficient CNTs nucleation sites then facilitate the crystallization of UHMWPE molecules into poor crystals with low melting temperatures during the gel-spinning process.

On the other hand, it is worth noting that the melting temperatures of the UHMWPE/CNTs as-prepared fiber series spun at 170°C reached the maximum as the as-prepared fiber was prepared from the solution with the 20 kg/m^3 optimum concentration (see Fig. 2). The melting temperatures reduce significantly as they were prepared from solution concentrations deviated from the optimum value. For instance, the melting temperatures of $F_{20}C_{0\text{-}170}$, $F_{20}C_{0.002\text{-}170}$ and $F_{20}C_{0.005\text{-}170}$ as-prepared fibers are 137.1, 135.7, and 135.3°C, which are about 2–3°C higher than those of the corresponding as-prepared fibers prepared from 15 and 25 kg/m^3 concentration (i.e., $F_{15}C_{0\text{-}170}$, $F_{15}C_{0.002\text{-}170}$, $F_{15}C_{0.005\text{-}170}$, and $F_{25}C_{0\text{-}170}$, $F_{25}C_{0.002\text{-}170}$, $F_{25}C_{0.005\text{-}170}$ as-prepared specimens), respectively. Similar optimum concentration dependency of the melting temperatures was found on those of other UHMWPE/CNTs as-prepared fiber series spun at other temperatures (i.e., $F_{15}C_{x\text{-}160}$, $F_{20}C_{x\text{-}160}$, $F_{25}C_{x\text{-}160}$, and $F_{15}C_{x\text{-}180}$, $F_{20}C_{x\text{-}180}$, $F_{25}C_{x\text{-}180}$ as-prepared fiber specimens) (see Figs. 3 and 4). As shown in Figures 2–4, the optimum concentration corresponding to the highest melting temperature and crystallinity values of the as-prepared fiber series specimens spun at varying temperatures increase from 15 to 25 kg/m^3 as their spinning temperatures increase from 160 to 180°C. However, the melting temperature and percentage crystallinity values of $F_{20}C_{x\text{-}170}$ as-prepared fiber series spun from the optimum concentration and temperature (i.e., 20 kg/m^3 and 170°C) are higher than those as-prepared specimens (i.e., $F_{15}C_{x\text{-}160}$ and $F_{25}C_{x\text{-}180}$) spun from the optimum concentrations but at other temperatures (see Figs. 2–4).

Achievable draw ratios of the as-prepared UHMWPE and UHMWPE/CNTs fibers

Figures 5 and 6 summarize the achievable draw ratios of the UHMWPE and UHMWPE/CNTs as-prepared fibers prepared at varying compositions and spinning temperatures. It is interesting to note that the achievable draw ratios of each as-prepared UHMWPE fiber series spun at a fixed temperature approach a maximum value when they were prepared at concentrations close to an optimum value. Similar to those found in their melting temperature and crystallinity values described in the previous section, the optimum spinning temperatures of the as-prepared UHMWPE fiber series increase significantly with the concentrations of the UHMWPE gel

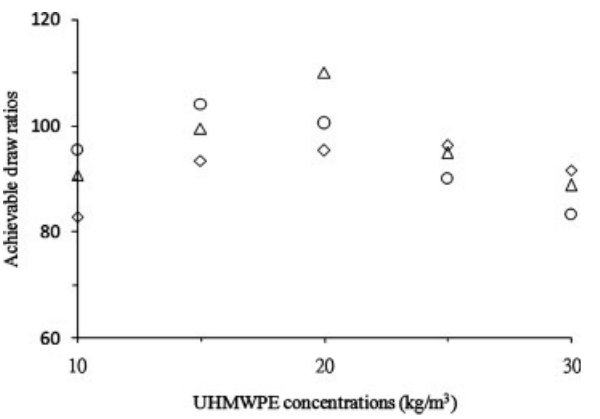

Figure 5 The achievable draw ratios of $F_xC_{0\text{-}160}$ (○), $F_xC_{0\text{-}170}$ (△), $F_xC_{0\text{-}180}$ (◇) fibers spun at varying UHMWPE concentrations.

solutions (see Fig. 5). As shown in Figure 5, the optimum concentrations increase from 15 to 20 and to 25 kg/m^3, as their spinning temperatures increase from 160 to 170 and to 180°C, respectively. These achievable draw ratios obtained for as-prepared UHMWPE fibers prepared near their optimum concentrations will be referred to as the optimum draw ratio (λ_{opT}) in the following discussion. It is worth noting that the λ_{opT} values of each as-prepared UHMWPE fiber series specimens spun at a fixed temperature reach another maximum, as their spinning temperature reaches around 170°C. As shown in Figure 5, the λ_{opT} values of as-prepared UHMWPE fibers spun at 170°C are about 70 and 180% higher than those of the as-prepared fibers spun at 160 and 180°C, respectively.

The λ_{opT} values of the as-prepared UHMWPE/CNTs as-prepared fiber series specimens (i.e., $F_{15}C_{x\text{-}160}$, $F_{20}C_{x\text{-}170}$, and $F_{25}C_{x\text{-}180}$ specimens) are summarized in Figure 6. It is worth noting that the λ_{opT} values of the as-prepared UHMWPE/CNTs fiber specimens are significantly higher than the λ_{opT} values of the corresponding as-prepared UHMWPE fiber series prepared at their optimum concentrations (i.e., $F_{15}C_{0\text{-}160}$, $F_{20}C_{0\text{-}170}$, and $F_{25}C_{0\text{-}180}$ fiber specimens), respectively. The achievable draw ratios of each $F_{15}C_{x\text{-}160}$, $F_{20}C_{x\text{-}170}$, and $F_{25}C_{x\text{-}180}$ as-prepared fiber series specimens increase with the CNTs contents and reach the maximum value as their CNTs contents reach the 0.002 wt % optimum value. Similar to those $F_{15}C_{0\text{-}y}$, $F_{20}C_{0\text{-}y}$, and $F_{25}C_{0\text{-}y}$ fiber series specimens, the maximum achievable draw ratios of $F_{15}C_{0.002\text{-}y}$, $F_{20}C_{0.002\text{-}y}$, and $F_{25}C_{0.002\text{-}y}$ as-prepared fiber specimens approach another maximum, as their spinning temperatures reach 170°C. For instance, the maximum achievable draw ratio of the $F_{15}C_{0.002\text{-}160}$, $F_{20}C_{0.002\text{-}170}$, and $F_{25}C_{0.002\text{-}180}$ fiber specimens reach about 119, 126, and 107, which are about 14.4, 14.2, and 11.7% higher than the achievable draw ratios of those $F_{15}C_{0\text{-}160}$, $F_{20}C_{0\text{-}170}$, and $F_{25}C_{0\text{-}180}$ fiber specimens without CNTs, respectively.

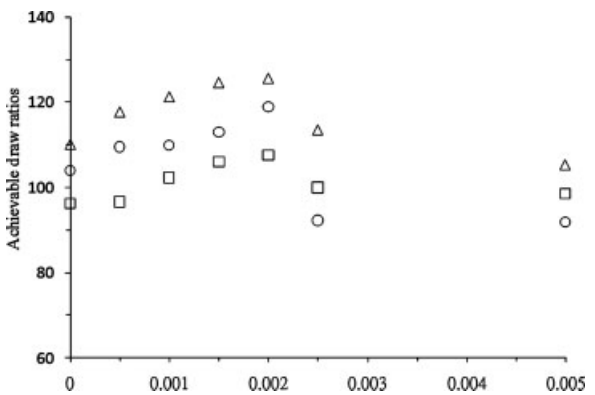

Figure 6 The achievable draw ratios of $F_{15}C_{x\text{-}160}$ (○), $F_{20}C_{x\text{-}170}$ (△), $F_{25}C_{x\text{-}180}$ (□) fibers with varying CNTs contents.

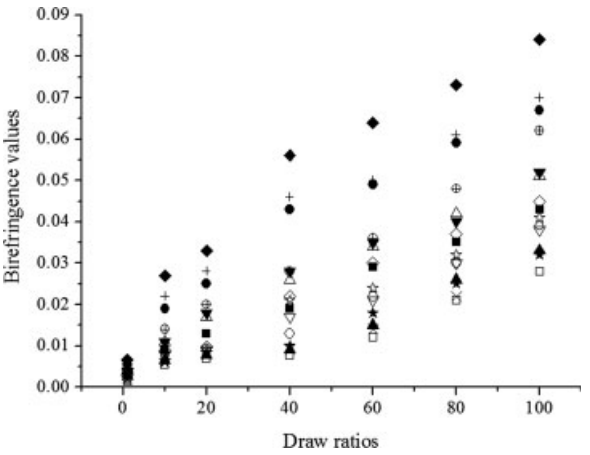

Figure 7 Birefringence values of $F_{15}C_{0\text{-}170}$ (○), $F_{15}C_{0.0010\text{-}170}$ (■), $F_{15}C_{0.0020\text{-}170}$ (▼), $F_{15}C_{0.0025\text{-}170}$ (◊), $F_{15}C_{0.0050\text{-}170}$ (☆), $F_{20}C_{0\text{-}170}$ (△), $F_{20}C_{0.0010\text{-}170}$ (●), $F_{20}C_{0.0020\text{-}170}$ (◆), $F_{20}C_{0.0025\text{-}170}$ (+), $F_{20}C_{0.0050\text{-}170}$ (⊕), $F_{25}C_{0\text{-}170}$ (□), $F_{25}C_{0.0010\text{-}170}$ (▲), $F_{25}C_{0.0020\text{-}170}$ (▽), $F_{25}C_{0.0025\text{-}170}$ (★), and $F_{25}C_{0.0050\text{-}170}$ (×) fibers drawn at varying draw ratios.

Birefringence properties of the as-prepared and drawn fibers

Typical birefringence properties of the as-prepared and drawn UHMWPE and UHMWPE/CNTs fiber specimens are summarized in Figures 7–10. As shown in Figure 7, the birefringence values of each as-prepared and drawn $F_{15}C_{x\text{-}170}$, $F_{20}C_{x\text{-}170}$, and $F_{25}C_{x\text{-}170}$ fiber series specimens spun at 170°C increase significantly with the increase in their draw ratios. Similar to those found for their achievable drawing properties, the birefringence values of each $F_{15}C_{x\text{-}170}$, $F_{20}C_{x\text{-}170}$, and $F_{25}C_{x\text{-}170}$ fiber series specimens with a fixed draw ratio increase consistently with increasing CNTs contents of gel solutions from which they were prepared, and reach the maximum as each fiber series specimens were prepared from the solution with the 0.002 wt % optimum CNTs content. At CNTs contents higher than the optimum value, the birefringence values of each $F_{15}C_{x\text{-}170}$, $F_{20}C_{x\text{-}170}$, and $F_{25}C_{x\text{-}170}$ fiber series specimens with a fixed draw ratio reduce significantly with increasing CNTs contents. Similar CNTs content dependency of the birefringence values was found on other UHMWPE/CNTs fiber series specimens (i.e., $F_{15}C_{0.002\text{-}160}$ and $F_{25}C_{0.002\text{-}180}$) spun from other optimum concentrations and temperatures (see Figs. 8 and 9). However, at a fixed draw ratio, the $F_{20}C_{0.002\text{-}170}$ as-prepared and drawn fiber series specimens spun from the optimum concentration and temperature exhibited higher birefringence values than those of corresponding $F_{15}C_{0.002\text{-}160}$ and $F_{25}C_{0.002\text{-}180}$ fiber series specimens spun from other optimum concentrations

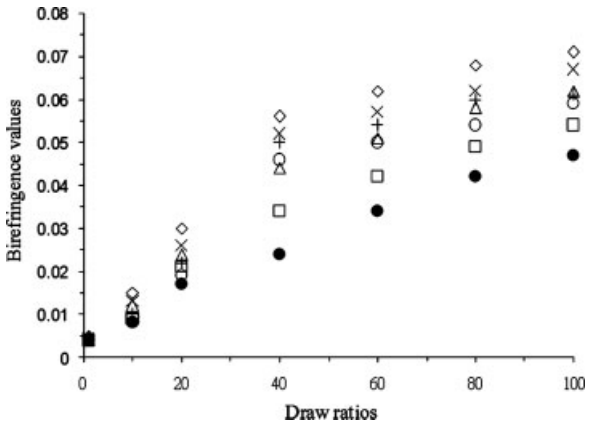

Figure 8 Birefringence values of $F_{15}C_{0\text{-}160}$ (●), $F_{15}C_{0.0005\text{-}160}$ (□), $F_{15}C_{0.0010\text{-}160}$ (△), $F_{15}C_{0.0015\text{-}160}$ (×), $F_{15}C_{0.0020\text{-}160}$ (◊), $F_{15}C_{0.0025\text{-}160}$ (+), and $F_{15}C_{0.005\text{-}160}$ (○) fibers drawn at varying draw ratios.

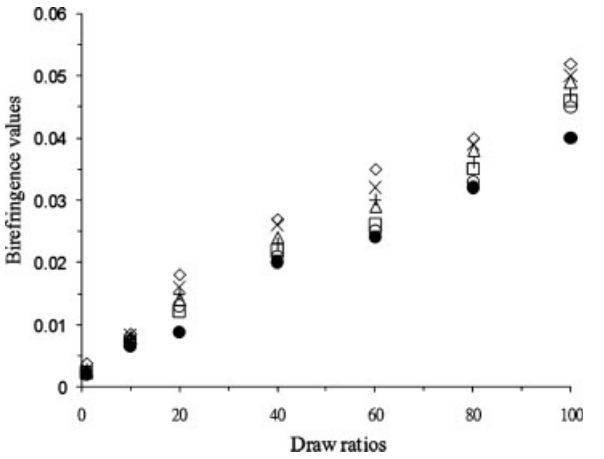

Figure 9 Birefringence values of $F_{25}C_{0\text{-}180}$ (●), $F_{25}C_{0.0005\text{-}180}$ (□), $F_{25}C_{0.0010\text{-}180}$ (△), $F_{25}C_{0.0015\text{-}180}$ (×), $F_{25}C_{0.0020\text{-}180}$ (◊), $F_{25}C_{0.0025\text{-}180}$ (+), and $F_{25}C_{0.005\text{-}180}$ (○) fibers drawn at varying draw ratios.

and temperatures (i.e., 15 kg/m^3/160°C and 25 kg/m^3/180°C) (see Fig. 10). On the other hand, it is interesting to note that the birefringence values of the $F_xC_{0.002\text{-}170}$ as-prepared or drawn fiber series specimens with a fixed draw ratio reached the maximum as they were prepared from the solution with the 20 kg/m^3 optimum concentration. As shown in Figure 7, at a draw ratio of 60, the birefringence value of $F_{20}C_{0.002\text{-}170}$ drawn fiber is about 82.9 and 204.8% higher than those of the $F_{15}C_{0.002\text{-}170}$ and $F_{25}C_{0.002\text{-}170}$ drawn fibers, respectively. Moreover, the $F_{20}C_{0.002\text{-}x}$ as-prepared and drawn fibers with a fixed draw ratio always exhibited the highest birefringence values as their spinning temperature reached the optimum spinning temperature at 170°C (see Fig. 10). Similar temperature dependency of the birefringence values was found on those of other UHMWPE/CNTs fiber series specimens (i.e., $F_{15}C_{0.002\text{-}x}$ and $F_{25}C_{0.002\text{-}x}$) prepared at other concentrations (See Fig. 10).

These results clearly suggest that the CNTs contents, UHMWPE concentrations and spinning temperatures have a significant influence on the achievable drawing properties of the as-prepared UHMWPE/CNTs fiber specimens and the corresponding birefringence properties of the as-prepared and drawn UHMWPE/CNTs fiber specimens. Presumably, the elongational stresses during the spinning processes can not easily orient the highly viscous and overly entangled UHMWPE/CNTs gel-network-structures of UHMWPE/CNTs gel solutions, when they were prepared with inappropriate compositions and/or spinning conditions (e.g., high UHMWPE concentrations and low spinning temperatures). It is generally understood that the achievable drawability of the gel fiber specimens can reach the maximum, when they were prepared near their critical concentrations, in which the numbers of entanglements in the coherent network structure of the gel fibers are not too many or too few to yield the maximum extension of UHMWPE during the gel deformation process. The entanglement numbers present in the gel-network-structure of gel solutions are expected to increase significantly as their gel concentrations increase. The relatively high entanglement numbers can be reduced to some extent at higher temperatures during the spinning process, because elongational stretching and disentangling of the gel solutions can occur more easily at higher temperatures during the spinning process than those fiber specimens spun at lower temperatures.[12,13] As a consequence, UHMWPE and/or UHMWPE/CNTs fibers prepared from higher gel concentrations should be spun at higher temperatures to yield the optimum numbers of entanglements in the coherent network structure of the gel fibers and to yield the

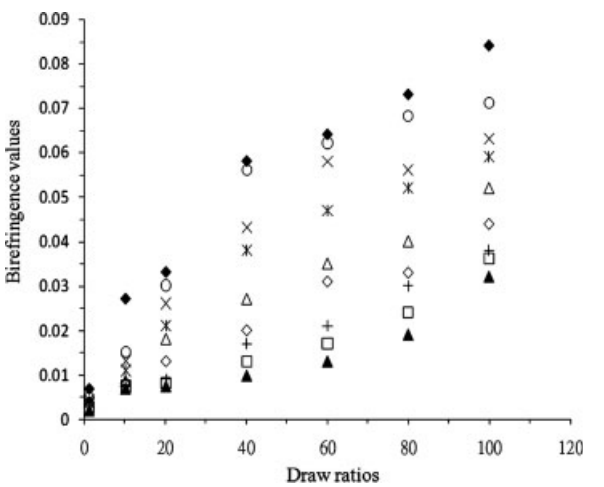

Figure 10 Birefringence values of $F_{15}C_{0.002\text{-}160}$ (○), $F_{15}C_{0.002\text{-}170}$ (*), $F_{15}C_{0.002\text{-}180}$ (□), $F_{20}C_{0.002\text{-}160}$ (×), $F_{20}C_{0.002\text{-}170}$ (◆), $F_{20}C_{0.002\text{-}180}$ (◊), $F_{25}C_{0.002\text{-}160}$ (▲), $F_{25}C_{0.002\text{-}170}$ (+), $F_{25}C_{0.002\text{-}180}$ (△) fibers drawn at varying draw ratios.

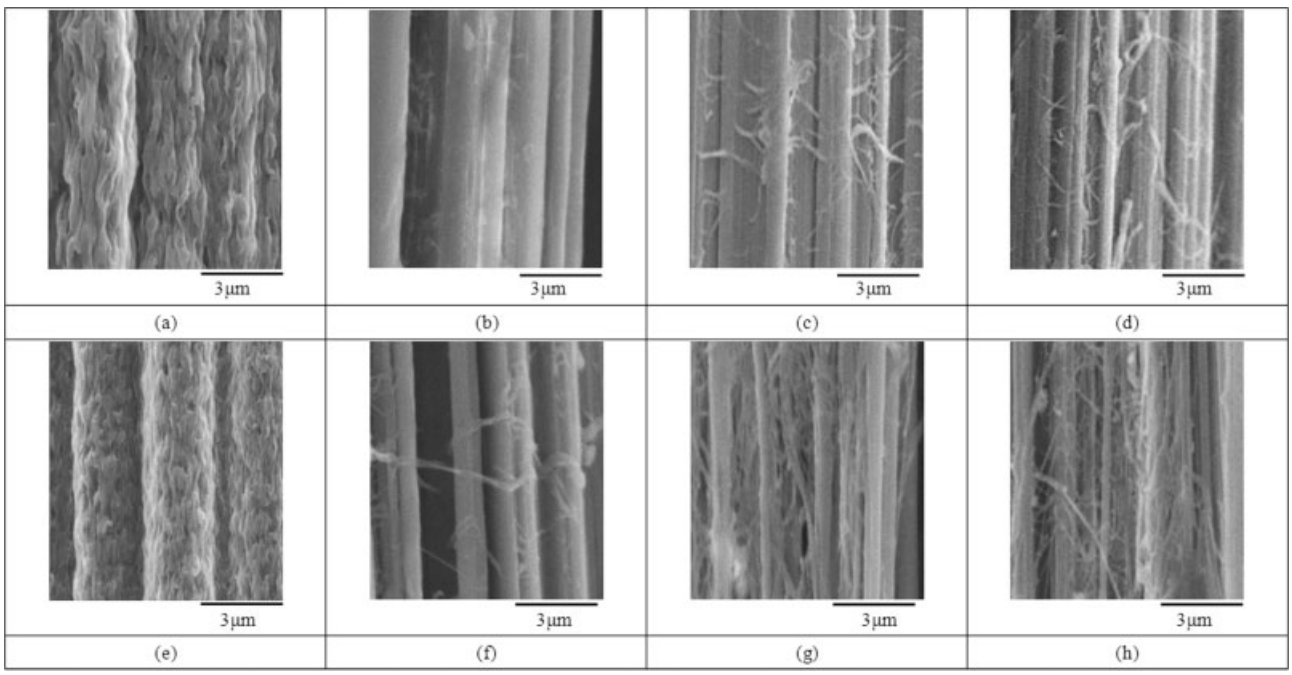

Figure 11 Scanning electron micrographs of the $F_{20}C_{0\text{-}170}$ fiber specimen with a draw ratio of (a) 1, (b) 20, (c) 60, and (d) 100; and $F_{20}C_{0.002\text{-}170}$ fiber specimen with a draw ratio of (e) 1, (f) 20, (g) 60, and (h) 100.

maximum achievable draw ratios and birefringence values during their gel deformation processes.

However, it is not completely clear what accounts for the interesting CNTs content dependency of the achievable drawing and birefringence properties found in the UHMWPE/CNTs as-prepared fibers. As evidenced by DSC analysis in the previous section, the peak melting temperatures and percentage crystallinity values of UHMWPE/CNTs as-prepared fibers reduce and increase significantly as their CNTs contents increase, respectively. These results suggest that the crystal perfection present in UHMWPE/CNTs as-prepared fibers reduce with increasing CNTs contents, although the amounts of less perfect crystals increase significantly as their CNTs contents increase. Presumably, the UHMWPE molecules can be more easily unfolded and pulled out from the less perfect crystal lamellae into oriented molecules than those from the more perfect crystal lamellae with higher melting temperatures. However, the amount of coagulated CNTs is likely to increase significantly when their CNTs contents are higher than certain values. These coagulated CNTs can slide with each other and serve as the defects during the drawing processes of UHMWPE/CNTs as-prepared fibers, and hence lead to a significant reduction in their achievable draw ratios and birefringence values. Based on these premises, it is reasonable to conclude that the achievable draw ratios of UHMWPE/CNTs as-prepared fibers and birefringence values of the UHMWPE/CNTs fibers with a fixed draw ratio reduce significantly when their CNTs contents are higher than the specific optimum CNTs contents.

SEM morphology analysis

Typical SEM micrographs of the as-prepared and drawn UHMWPE and UHMWPE/CNTs fibers are shown in Figure 11. Many demarcated drawn "micro-fibrils" were found paralleling the drawing direction of the drawn UHMWPE and/or UHMWPE/CNTs fiber specimens as their draw ratios increase, wherein the thicknesses of these drawn "micro-fibrils" reduce significantly as their draw ratios increase. Moreover, it is worth noting that more drawn fibril debris and thinner "micro-fibrils" were found on the etched surfaces of UHMWPE/CNTs fibers than those of the base UHMWPE fibers with the same draw ratios, respectively [see Fig. 11(d,e,f)].

It is not completely clear what accounts for the interesting demarcated "micro-fibril" morphology found in the UHMWPE/CNTs drawn fiber specimens. Presumably, during the ultra-drawing processes, many of the UHMWPE crystals with relatively poor perfection can be unfolded and pulled out of the crystal lamellae of UHMWPE/CNTs fibers in an easier way than those more perfect crystals present in base UHMWPE fiber specimens. The unfolded UHMWPE molecules pulled out from the crystal lamellae of UHMWPE/CNTs fibers can then

gradually transform into the oriented "micro-fibrils" during their ultra-drawing processes. It is, therefore, understandable that more demarcated "micro-fibril" morphology was found in the drawn UHMWPE/CNTs fiber specimens than those found in the corresponding drawn UHMWPE fiber specimens.

Tensile properties of as-prepared and drawn UHMWPE/CNTs fibers

As shown in Figures 12 and 13, the tensile strength and moduli of UHMWPE and UHMWPE/CNTs fiber specimens improve consistently as their draw ratios increase. In a way similar to what was observed for the birefringence and achievable drawing properties, the tensile strengths and moduli of the UHMWPE/CNTs fibers prepared at the optimum CNTs contents, UHMWPE concentrations and/or spinning temperatures are significantly higher than those of fibers prepared at other compositions, spinning temperatures but stretched to the same draw ratio. For instance, at a draw ratio of 20, the tensile strength and modulus of $F_{20}C_{0.002\text{-}170}$ fiber prepared at the optimum CNTs content, UHMWPE concentration, and spinning temperature are about 17% higher than those of drawn $F_{20}C_{0\text{-}170}$ fiber, fibers prepared at the same concentration and spinning temperature but zero CNTs content (see Figs. 12 and 13). It is generally believed that the tensile properties of the drawn specimens depend primarily on the degree of orientation of the drawn specimens, as their molecular weights are constant.[14,15] As described previously, the $F_{20}C_{0.002\text{-}170}$ as-prepared and/or drawn fibers always exhibited higher birefringence value than other fibers prepared at other compositions and conditions but the same draw ratio. These results clearly suggest that a good orientation of UHMWPE molecules along the drawing

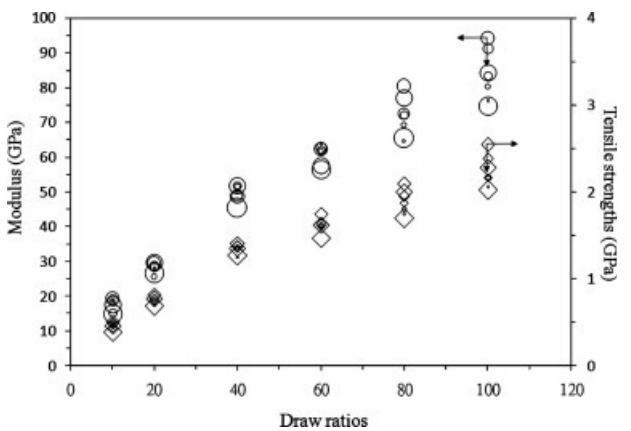

Figure 12 Tenacity and modulus values of $F_{20}C_{0\text{-}170}$ (◇,○), $F_{20}C_{0.0005\text{-}170}$ (◇,○), $F_{20}C_{0.0010\text{-}170}$ (◇,○), $F_{20}C_{0.0015\text{-}170}$ (◇,○), $F_{20}C_{0.0020\text{-}170}$ (◇,○), $F_{20}C_{0.0025\text{-}170}$ (◇,○), and $F_{20}C_{0.005\text{-}170}$ (◇,○) fibers drawn at varying draw ratios.

z

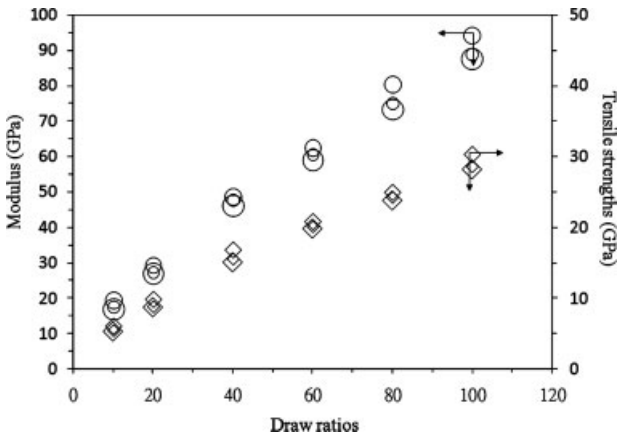

Figure 13 Tenacity and modulus values of $F_{15}C_{0.002\text{-}160}$ (◇,○), $F_{20}C_{0.002\text{-}170}$ (◇,○), $F_{25}C_{0.002\text{-}180}$ (◇,○) fibers with varying draw ratios.

direction has a positive influence on the tensile properties of the UHMWPE/CNTs fibers, which can be obtained by preparing the fibers at the optimum CNT content, UHMWPE concentration, and spinning temperature.

CONCLUSIONS

The CNTs contents, UHMWPE concentrations, and spinning temperatures were found to have a significant influence on the shear viscosities, spinnable properties of the UHMWPE/CNTs gel solutions. As expected, the shear viscosities of spinnable UHMWPE gel solutions increase significantly with the increase in UHMWPE concentrations. Tremendously high shear viscosities (η_s) of UHMWPE gel solutions were found as the temperatures reached 140°C, at which their η_s values approached the maximum. After adding CNTs, the η_s values of UHMWPE/CNTs gel solutions increase significantly and reach the maximum as their CNTs contents increase up to an optimum value of 0.002 wt %. Similar CNTs content dependence of the achievable draw ratio and birefringence values of the as-prepared and drawn UHMWPE/CNTs fibers was found. In fact, the achievable draw ratios of UHMWPE/CNTs as-prepared fibers prepared at optimum CNTs and UHMWPE composition and spinning temperature are about 15–30% higher than those of the corresponding UHMWPE as-prepared fibers prepared at the optimum concentration. As evidenced by DSC analysis, the percentage crystallinity and melting temperature values of the as-prepared UHMWPE/CNTs fibers increase and reduce significantly as their CNTs contents increase, respectively. Presumably, the UHMWPE molecules can be more easily unfolded and pull out from the less

perfect crystal lamellae with lower melting temperatures into oriented molecules and/or "micro-fibrils" than those from the more perfect crystal lamellae with higher melting temperatures. As a consequence, more demarcated "micro-fibril" morphology was found for the drawn UHMWPE/CNTs fiber specimens than those found for the corresponding drawn UHMWPE fiber specimens with the same draw ratios. However, the amounts of coagulated CNTs are likely to increase significantly as their CNTs contents are higher than certain specific values. These coagulated CNTs can slide with each other and serve as the defects during the drawing processes of UHMWPE/CNTs as-prepared fibers, and hence lead to a significant reduction in their achievable draw ratios and birefringence values. Finally, in a way similar to those found for the birefringence and achievable drawing properties, a good orientation of UHMWPE molecules along the drawing direction has a beneficial influence on the tensile properties of the UHMWPE/CNTs fibers, which can be obtained by preparing the fibers at the optimum CNTs content, UHMWPE concentration, and spinning temperature.

References

1. Iijima, S. Nature 1991, 354, 56.
2. Andrew, R.; Jacques, D.; Rao, A. M.; Rantell, T.; Derbyshire, F.; Chen, Y. J Appl Polym Sci 1999, 75, 1329.
3. Qian, D.; Dickey, E. C.; Andrews, R.; Rantell, T. J Appl Polym Sci 2000, 76, 2868.
4. Vigolo, B.; Penicaud, A.; Coulon, C.; Sauder, C.; Pailler, R.; Journet, C.; Bernier, P.; Poulin, P. Science 2000, 290, 1331.
5. Dalton, A. B.; Collins, S.; Munoz, E.; Razal, J. M.; Ebron, V. H.; Ferraris, J. P.; Coleman, J. N.; Kim, B. G.; Baughman, R. H. Nature 2003, 423, 703.
6. Kearns, J. C.; Shambaugh, R. L. J Appl Polym Sci 2002, 86, 2079.
7. Wang, Y.; Cheng, R.; Liang, L.; Wang, Y. Compos Sci Tech 2005, 65, 793.
8. Ruan, S.; Gao, P.; Yu, T. X. Polymer 2006, 47, 1604.
9. Mao, Z.; Garg, A.; Sinnott, S. B. Nanotechnology 1999, 10, 273.
10. Wagner, H. D. Chem Phys Lett 2002, 361, 57.
11. Wunderlich, B. Macromolecular Physics; Academic Press: New York, 1973; Vol. 1, p 388.
12. Yeh, J. T.; Chang, S. S. Polym Eng Sci 2002, 42, 1558.
13. Jiang, T.; Yeh, J. T.; Lin, Y. T.; Chen, K. N. Polym Eng Sci 2003, 43, 1765.
14. Matsuo, M.; Sawatari, C.; Iida, M.; Yoneda, M. Polym J 1985, 17, 1197.
15. Kanamoto, T.; Tsurta, A.; Tanana, K.; Takeda, M.; Porter, R. S. Macromolecules 1988, 21, 470.